

# Comprehensive aerial survey quantifies high methane emissions from the New Mexico Permian Basin

Yuanlei Chen,<sup>\*,†,§</sup> Evan D. Sherwin,<sup>†,§</sup> Elena S.F. Berman,<sup>‡</sup> Brian B. Jones,<sup>‡</sup>  
Matthew P. Gordon,<sup>‡</sup> Erin B. Wetherley,<sup>‡</sup> Eric A. Kort,<sup>¶</sup> and Adam R. Brandt<sup>†</sup>

<sup>†</sup>*Energy Resources Engineering, Stanford University, Stanford, CA 94305, USA*

<sup>‡</sup>*Kairos Aerospace, Mountain View, CA 94040, USA*

<sup>¶</sup>*Climate and Space Sciences and Engineering, University of Michigan, Ann Arbor, MI 48109, USA*

<sup>§</sup>*Denotes equal contribution*

E-mail: [yuliac@stanford.edu](mailto:yuliac@stanford.edu)

## Abstract

Limiting emissions of climate-warming methane from oil and gas (O&G) is a major opportunity for short-term climate benefits. We deploy a basin-wide airborne survey of the New Mexico Permian Basin, spanning 35,923 km<sup>2</sup>, 26,292 active wells, and over 15,000 km of natural gas pipelines using an independently-validated hyperspectral methane point source detection and quantification system. The airborne survey repeatedly visited over 90% of the active wells in the survey region throughout October 2018 to January 2020, totaling 117,658 well visits. We estimate total O&G methane emissions in this area at 194 (+72/-68, 95% CI) metric tonnes per hour (t/h), or 9.4% (+3.5%/-3.3%) of gross gas production. 50% of observed emissions come from

12 large emission sources with persistence-averaged emission rates over 308 kg/h. This re-  
13 sult emphasizes the importance of capturing low-probability, high-consequence events  
14 through basin-wide surveys when estimating regional O&G methane emissions.

## 15 **Keywords**

16 Methane emissions, oil and gas, leakage, hyperspectral imaging, remote sensing, airborne  
17 survey

## 18 **Synopsis**

19 Surveying nearly every oil and gas asset in a region substantially increases estimates of total  
20 emissions of climate-warming methane.

## 21 **Introduction**

22 Methane, the primary constituent of natural gas (NG), is a potent greenhouse gas (GHG)  
23 with a global warming potential at least 30 times larger than carbon dioxide.<sup>1</sup> While the  
24 transition to renewable energy is accelerating, inertia in industrial systems and the need  
25 for stable energy supply means that NG will continue to be used for decades. Therefore,  
26 reducing the GHG intensity of oil and gas (O&G) through preventing methane emissions is  
27 an important mitigation opportunity.

28 The Permian Basin in Texas and New Mexico produces more oil than all but five countries  
29 in the world.<sup>2</sup> Over the past decade, Permian oil production has quadrupled and gas produc-  
30 tion has tripled.<sup>2</sup> However, as production from this oil-rich basin has increased, incentives to  
31 limit the resulting emissions of climate-warming methane have been lacking. Economically,  
32 operators view oil as the primary product,<sup>3</sup> because natural gas prices in the region have  
33 remained low – or sometimes even negative – due in part to a lack of gas takeaway capacity.<sup>4</sup>

34 Regulations have also been slow to catch up to the pace of development – New Mexico in  
35 particular has never before had large-scale oil production, and is only now implementing  
36 state-level regulations on venting and flaring.<sup>5</sup> Taken together, the lack of economic and  
37 regulatory incentives to reduce methane emissions has likely contributed to high methane  
38 emissions in the Permian Basin.<sup>6–8</sup>

39 A number of studies have found abnormally high methane emissions from O&G opera-  
40 tions in the Permian Basin. With aircraft- and tower- based methane concentration mea-  
41 surements, Lyon et al. estimated the NG production loss at 3.3% in a subdomain of the  
42 Permian.<sup>7</sup> Zhang et al. and Schneising et al. apply inversion methods based on satellite  
43 measurements, finding a NG production loss rate of roughly 3.7% for the full Texas and  
44 New Mexico Permian.<sup>6,9</sup> More recently, a hyperspectral airborne survey by Cusworth et  
45 al. characterizes the very heavy tail of site-level methane emissions in the Permian Basin,  
46 finding 2,874 methane plumes above 100 kg/h and 457 above 1,000 kg/h, larger than any  
47 observation previously found in ground-based methane surveys.<sup>10</sup> Because of the different  
48 methods and coverage areas of these studies, direct comparison of their results is challenging  
49 and uncertainty remains about the emissions rates in the Permian Basin.

50 However, these studies consistently find emissions significantly in excess of government  
51 estimates. The US Environmental Protection Agency (EPA) Greenhouse Gas Inventory  
52 (GHGI) estimates a national NG production loss rate of 1.5%.<sup>11,12</sup> But the GHGI has been  
53 identified as a conservative estimate of methane emissions,<sup>11,13,14</sup> and a recent alternative  
54 estimate finds a US national average NG production loss rate of 2.3% based on a synthesis  
55 of measurements from across the O&G supply chain.<sup>11</sup> Note that the Permian findings are  
56 even higher than this adjusted national average. One possible driver of even larger emissions  
57 in the Permian might be the large leaks found by Cusworth et al.: infrequent large leaks  
58 (so-called “super-emitters”) are thought to play an important role in driving total emissions.  
59 Across many studies, the top 5% of leaks contribute over 50% of emissions.<sup>15</sup>

60 How are these figures still so uncertain? In short: field measurements are noisy and

61 the high expense of surveys means that most studies to date have been very data-limited.  
62 For example: the largest multi-paper synthesis dataset of ground-based site-level methane  
63 measurements includes measurements from  $\sim 1000$  well sites across 5 different studies.<sup>13</sup>  
64 Given that there are over one million active O&G wells in the US, this is a relatively small  
65 sample size. Especially given the importance of infrequent super-emitters in driving total  
66 emissions, such sample sizes are difficult to extrapolate.

67 We bridge this gap using a novel approach: A basin-wide aerial survey capable of mea-  
68 suring emissions from nearly every asset in an O&G producing region with an instrument  
69 capable of quantifying and attributing medium-to-large point-source emissions. This work  
70 allows us to identify emissions larger than any documented in ground-based surveys, and to  
71 obtain sample sizes orders of magnitude larger than prior approaches.

## 72 **Materials and Methods**

### 73 **Repeated comprehensive airborne survey**

74 We use a basin-wide dataset from aerial surveys performed by Kairos Aerospace (henceforth  
75 “Kairos”) to evaluate medium-to-large point-source emissions in the New Mexico Permian  
76 Basin. Kairos’ technology consists of an integrated infrared imaging spectrometer, optical  
77 camera, global positioning system (GPS), and inertial motion unit.<sup>16</sup> The instrument is  
78 flown on an airborne platform at  $\sim 900$  m above ground, and generates methane plume  
79 images superimposed over concurrent optical images (see example in Figure 1a).

80 Sherwin, Chen et al. evaluated the Kairos technology by conducting an independent,  
81 single-blind test of the system including 234 total measurements. They found 1) no false  
82 positives; 2) a minimum detection level of 5 kg of methane per hour per meter per second of  
83 wind (kg/h/mps) and a partial detection range of 5-15 kg/h/mps; and 3) an  $R^2$  value of 0.84  
84 between the measured and actual release volumes across a wide range of release sizes tested  
85 (18-1025 kg/h) above the technology’s detection limit. This study showed the technology’s

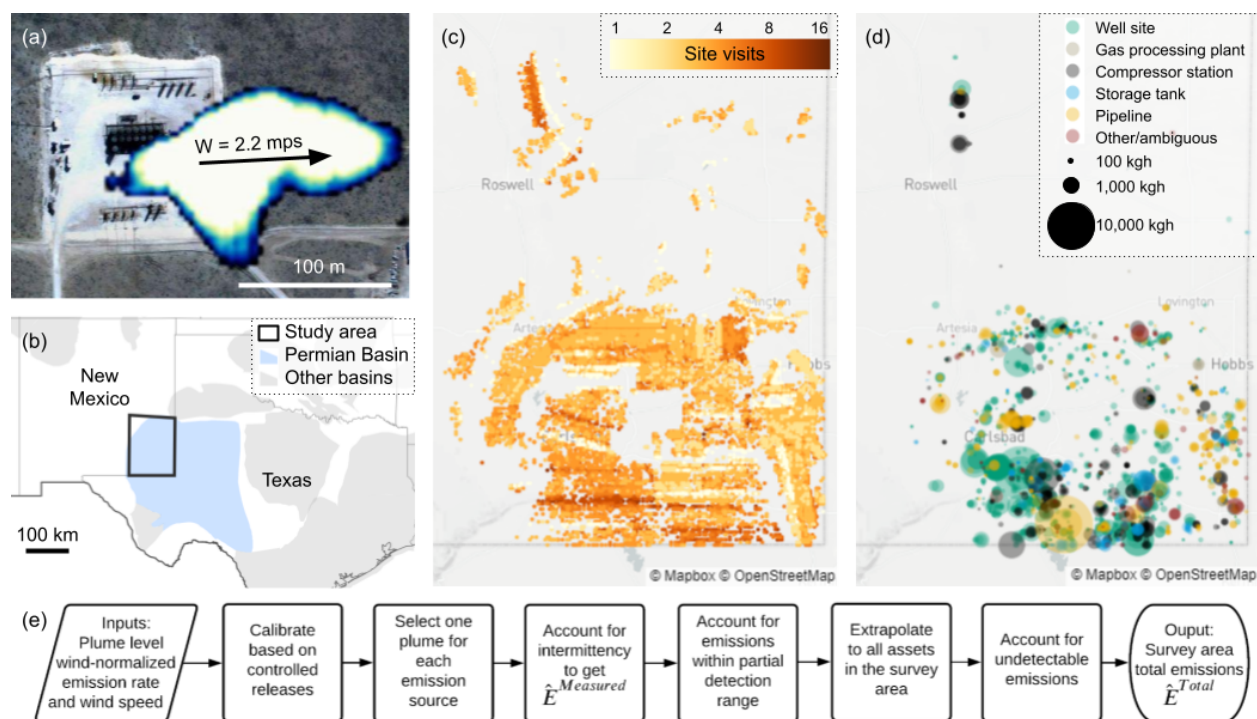


Figure 1: Methane emission data and analysis workflow. (a) Methane plume from an O&G site. White pixels indicate a high probability of excess methane. (b) Permian Basin map with the survey area outlined in black. Other sedimentary basins are colored grey.<sup>17</sup> (c) Number of measurements of each point asset (pipelines not included). The colorbar is on a logarithmic scale. (d) 1,985 detected methane plumes colored by asset type and scaled by plume size. (e) Analysis workflow for estimating survey area total emissions based on methane plume observations.

86 ability to quantify super-emitters in the field.<sup>18</sup> See the Supplementary Information (SI),  
 87 Section S1 for detailed controlled release results.

88 The Kairos survey of the New Mexico Permian was conducted over 115 flight days from  
 89 October 2018 to January 2020 (Figure 1b). The campaign surveyed 35,923 km<sup>2</sup> (13,870 sq.  
 90 mi.) and 26,292 active wells, or 91.2% of all active wells in the covered region. All data were  
 91 anonymized using procedures described in the SI, Section S2.2.

92 Each surveyed non-pipeline facility was observed an average of 4 times. Accounting for  
 93 these repeated measurements, a total of 117,658 visits to wells were performed. Figure 1c  
 94 shows the number of measurements of each point asset (non-pipeline). Multiple overflights  
 95 also allowed for more frequent sampling in the temporal dimension and provided insights into

96 emission intermittency. The SI, Section S2 details the flight plans and Section S3 presents  
97 an analysis of intermittency.

## 98 **Basin-wide emissions quantification**

99 A methane survey will detect some number of plumes, each of which is associated to an emis-  
100 sion source. An emission source is defined as a point coordinate with one or more methane  
101 plumes observed during the campaign. The SI, Section S4.2 describes the association process.

102 Figure 1e illustrates the analysis workflow to derive survey-area total emissions. The SI,  
103 Section S5.1 describes each step in detail. For each plume, Kairos reports a wind-independent  
104 emission rate in kgh/mps, and we multiply this rate with the National Oceanographic and  
105 Atmospheric Administration’s High Resolution Rapid Refresh (HRRR) wind speed reanalysis  
106 estimate at the imaging time and plume coordinates to calculate emission rate in kg/h for  
107 each plume using the method described in Duren et al.<sup>19</sup>

108 We then refer to the the single-blind test of the instrument by Sherwin, Chen et al. to  
109 determine the instrument’s detection limit and quantification accuracy and precision (see the  
110 SI, Section S1). Data from the single-blind test shows the instrument’s apparent overestima-  
111 tion tendency for larger releases, possibly due to an underlying nonlinearity or a boundary  
112 bias for calibration (see the SI, Section S1.6). Using a sublinear correlation from the single-  
113 blind test, we calibrate the plume-level emission rates in kg/h. The single-blind test also  
114 quantified the measurement uncertainties, which is modeled as a fixed percent error distri-  
115 bution at all emission levels, indicating that the modeled absolute error scales linearly with  
116 emission magnitude (see the SI, Section S1.5). To account for the measurement error in  
117 the New Mexico Permian Basin study, we assume that the percent error follows a normal  
118 distribution and apply this error to the plume-level emission rates with 1000 Monte Carlo  
119 realizations.

120 For each realization of the Monte Carlo approach, we then select one plume for each  
121 emission source if multiple plumes were observed during repeated overflights. Then we

122 multiply the selected plume quantification with a binary term to account for intermittency.  
123 The binary term is modeled to follow a Bernoulli distribution with  $p$  equal to fraction of  
124 overflights that observed emissions at each emission source. Basin-wide directly-measured  
125 emission ( $\hat{E}^{Measured}$ ) is the sum of all emission source level emissions after accounting for  
126 intermittency. The SI, Section S3 explains why this is an unbiased estimate of total measured  
127 emissions.

128 To account for undetected emissions in the partial detection range of Kairos' technology,  
129 we add to  $\hat{E}^{Measured}$  the expected amount of emissions undetected within the partial detec-  
130 tion range based on both the detection probabilities and what was observed in the partial  
131 detection range during the New Mexico Permian campaign (see the SI, Section S1 and S5.1).  
132 We then scale up the estimate to the full study area, the black polygon in Figure 1, assuming  
133 that emissions in uncovered areas scale with the number of O&G wells in the area.

134 Below Kairos' minimum detection threshold, we assume that emissions are described by  
135 a combination of the fractional loss rate from Alvarez et al. of 2.2% for production and  
136 midstream as well as the emission size distribution from Omara et al.<sup>11,13</sup> Assuming winds  
137 from the New Mexico Permian, Kairos would be able to detect 63% of emissions from Omara  
138 et al. 2018, translating to a fractional loss rate of 0.8% for emissions below the detection  
139 threshold in this study. See the SI, Section S1.4 and S5.1 for partial detection definition  
140 and detailed steps to account for undetected emissions. We denote the total emissions after  
141 incorporating undetected emissions as  $\hat{E}^{Total}$ .

## 142 **Results and Discussion**

### 143 **Large basin-wide methane emissions quantified**

144 The campaign detected 1985 methane plume observations from 958 distinct emission sources,  
145 indicating that for the average emissions source, approximately two different overflights  
146 observed a plume. Using the approach described in Materials and methods, our estimate

147 for measured emissions ( $\hat{E}^{Measured}$ ) from the New Mexico Permian is 153 (+71/-70, 95%  
 148 CI) metric tonnes per hour (t/h), shown as the left bar in Figure 2a. This corresponds to  
 149  $7.4\% \pm 3.4\%$  of gross gas production in the full survey area.

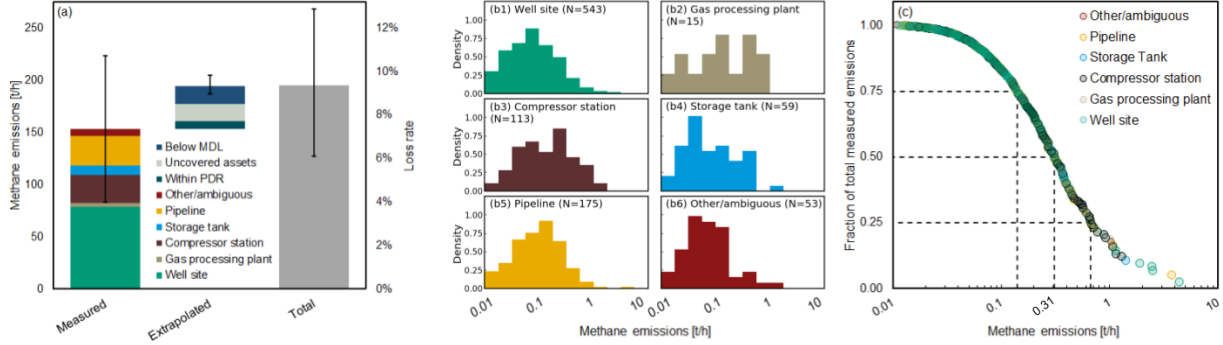


Figure 2: Persistence-averaged emissions. (a) The left bar shows directly measured methane emissions ( $\hat{E}^{Measured}$ ) broken down by asset type. The error bars indicate 95% confidence intervals. The middle bar breaks down extrapolated emissions into undetected emissions within the partial detection range (PDR), emissions from assets not measured in the survey area, and emissions that are below minimum detection limit (MDL). The right bar shows that the estimate of total methane emissions in the survey area from upstream and midstream O&G operations is 194 (+72/-68) t/h, 9.4% (+3.5%/-3.3%) of gross gas production. (b) The distribution of asset-type-specific persistence-averaged emission source sizes, which follow heavy-tailed distributions. (c) Cumulative emission fraction as a function of persistence-averaged emission source sizes.

150 Accounting for partial detection, emissions below minimum detection limit, and scaling  
 151 up to assets not covered in this aerial campaign, the total survey area emission estimate  
 152 ( $\hat{E}^{Total}$ ) is 194 (+72/-68) t/h, equivalent to 9.4% (+3.5%/-3.3%) of gross gas production.

153 A breakdown of  $\hat{E}^{Measured}$  by emission source asset type reveals that  $79 \pm 46$  of the 153 t/h  
 154 of measured emissions comes from well sites. A “well site” is defined here as the ensemble  
 155 of all assets (including wells, gathering lines, storage tanks, and compressor stations) found  
 156 on a congruent gravel or concrete area containing at least one well. Midstream assets were  
 157 also a significant source, with  $29 \pm 20$  t/h emitted from pipelines (including underground gas  
 158 gathering pipelines) and  $26 \pm 16$  t/h emitted from compressor stations without a well on site.  
 159 The remainder was emitted from stand-alone storage tank sites ( $9 \pm 6$  t/h), gas processing  
 160 plants ( $4 \pm 2$  t/h), and other or ambiguous sources ( $7 \pm 4$  t/h). See the SI, Section S4.2 for



161 definitions of each asset type and the asset attribution method.

162 Figure 2b shows the distribution of persistence-averaged emission source sizes and indi-  
163 cates heavy-tailed distributions of emission sizes across asset types. As displayed in Figure  
164 2c, 50% of total emissions are from 118 ( $\sim 12\%$ ) of the 958 sources, those larger than 308 kg/h.  
165 The heavy tail gets even heavier for the largest emissions and contains a disproportionate  
166 number of midstream assets. The largest persistence-averaged emission source emits at 4.3  
167 t/h. The persistence of the heavy tail for distributions of large emissions demonstrates the  
168 significant potential for mitigating methane by detecting and fixing these high-consequence  
169 sources.

170 Sensitivity tests show robust support for a mean natural gas fractional loss rate of at  
171 least 8.1% of gas produced. As listed in Table 1, switching from a sublinear fit to a linear  
172 fit for the calibration step, described in the SI, Section S7, brings the loss rate estimate  
173 up to 10.2% (+4.1%/-3.6%). A linear fit forced through the origin leads to an estimate of  
174 11.0% (+5.0%/-4.6%). In the calibration fitting process, leaving out large controlled releases  
175 improves the statistical validity of the fit due to the underlying asymmetric error distribution  
176 at high emission rates, and also increases the total emission estimate, as described in the SI,  
177 Section S1.5. Using an alternative wind dataset (the commercial Dark Sky wind reanalysis  
178 product) results in comparable emissions estimates both for low- and high-time-resolution  
179 versions of the data.<sup>20</sup>

180 To provide a conservative estimate for the loss rate, we apply three additional sensitivity  
181 scenarios: 1) disallow extrapolation and assume that emission rates cannot exceed the largest  
182 controlled release rate (1025 kg/h); 2) exclude the top 20 largest plumes ( $\sim 1\%$  of the dataset);  
183 and 3) assume that there are no emissions from plumes below the Kairos minimum detection  
184 limit. These conservative approaches still result in mean loss rate estimates over 8% with a  
185 5<sup>th</sup> percentile estimate never falling below 5.2%.

186 These sensitivity cases show that even the lower-bound estimates of the conservative  
187 scenarios based on our basin-wide data are larger than estimates from other Permian studies:

Table 1: Survey-area total methane emission rate and loss rate estimates. Presented as a fraction of total methane production, for the base case and seven sensitivity cases.

Cases	$\hat{E}^{Total}$ (t/h)			%NG production loss		
	Mean	5 <sup>th</sup> %	95 <sup>th</sup> %	Mean	5 <sup>th</sup> %	95 <sup>th</sup> %
Base case	194	126	266	9.4%	6.1%	12.9%
Linear fit for calibration	212	136	296	10.2%	6.6%	14.3%
Linear fit forced through origin for calibration	228	131	335	11.0%	6.4%	16.0%
Cutoff at $1\sigma$ below max controlled release	216	137	301	10.4%	6.9%	14.6%
Dark Sky wind high time resolution	181	124	244	8.7%	6.1%	11.8%
Dark Sky wind low time resolution	217	142	301	10.4%	6.8%	14.3%
Disable extrapolation	167	119	220	8.1%	5.7%	10.6%
Exclude top 20 plumes	173	117	233	8.3%	5.5%	11.2%
No below minimum detection emissions	177	109	249	8.5%	5.2%	12.0%

188 3.7% by the Zhang et al. and Schneising et al. satellite-based top-down studies and 3.3%  
 189 by the Lyon et al. tower- and airplane-based top-down study, although these studies include  
 190 both Texas and New Mexico.<sup>6,7,9</sup> Applying our basin-wide quantification method to data  
 191 from Cusworth et al. in the overlapping region of New Mexico, we find a fractional loss  
 192 rate of 4.4% for directly-measured emissions.<sup>10</sup> This rises to 5.9% after accounting for an  
 193 evidently higher effective minimum detection threshold compared to the Kairos survey (see  
 194 the SI, Section S9).

## 195 Importance of large sample size and direct measurement

196 Figure 3 compares our results with Zhang et al., which uses a methane flux inversion approach  
 197 based on satellite data to calculate a NG production loss rate of  $3.7\% \pm 0.7\%$ , or 331 t/h in a  
 198 region of the Permian spanning both New Mexico and Texas. We apply spatial, time-of-day,  
 199 and study period alignment corrections (described in the SI, Section S8) to enable a more  
 200 direct comparison to our study results. These adjustments increase the estimate of Zhang  
 201 et al. from 64 t/h (in our study area) to 106 t/h. This is still below  $\hat{E}^{Measured}$ .

202 The remaining discrepancy may be due to various causes. First, their study focused on a  
 203 larger spatial domain and was not focused on NM Permian. Some modeling assumptions in

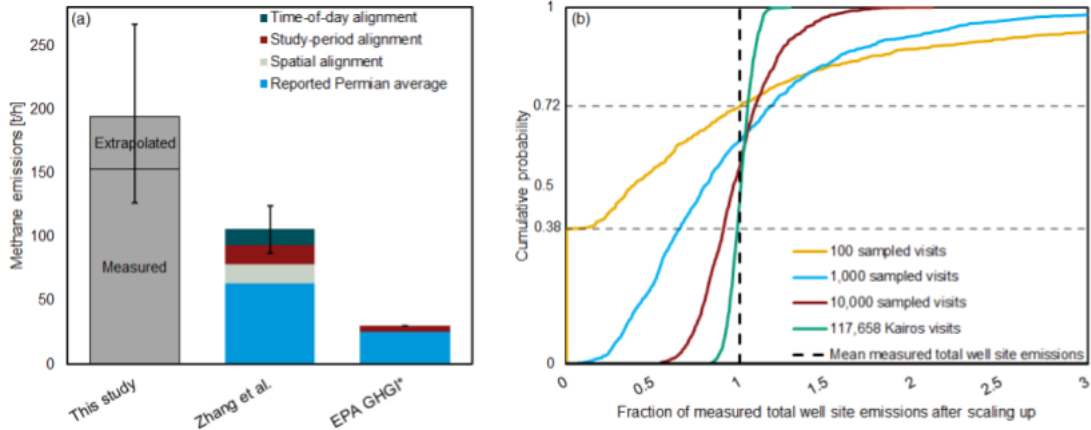


Figure 3: Comparison with other studies and the importance of large sample size for sampling from a heavy-tailed distribution. (a) Estimated methane emissions from the New Mexico Permian from this study (left bar), Zhang et al. posterior (middle bar), and EPA GHGI (right bar). Beige, grey, and red bars indicate adjustments performed by this study to better allow for direct comparison of results (see the SI, Section S8). \*Note that the EPA GHGI presented here is based on the gridded GHGI in,<sup>6</sup> which takes into account the production growth between the last official EPA GHGI publication in 2012 and the Zhang et al. study period. (b) Simulations showing the probability of under- or over-estimating total emissions if only a subset of the 117,658 well visits in this study were conducted. Surveying 100 wells generates a 72% chance of underestimating survey-area total emissions, while visiting 1000, 10,000, and 117,658 wells generates a 63%, 56%, and 50% chance of underestimation, respectively. The computed ratios of simulated emissions detection over mean Kairos-measured well site emissions are plotted on the x-axis.

204 Zhang et al. may also introduce conservatism (a conservative prior flux estimate and spatial  
 205 concentration of prior emissions at O&G production sites, as opposed to midstream assets).  
 206 We explore this comparison more in the SI, Section S8.

207 It is important to explore further a key strength of our method compared to prior studies:  
 208 very large study sample size. We explore this by simulating the impact of small sample sizes  
 209 on total emissions estimates (Figure 3b).

210 Suppose that we only visited 100 wells, a typical sample size for ground-based campaigns.  
 211 Based on a random subsample of 100 well visits from our full dataset of 117,658 effective  
 212 well visits, and using the same minimum detection limit as Kairos, this hypothetical 100-  
 213 well survey would detect no emissions 38% of the time and would find average emissions

214 lower than the basin-wide survey 72% of the time (based on 1000 Monte Carlo realizations).  
 215 Median emissions would be 38% our full survey estimate. In a small number of Monte Carlo  
 216 realizations (8%), scaling up the 100 sampled visits results in overestimates by a factor of two  
 217 or more. Over many Monte Carlo realizations, a sample size of 100 will ultimately converge  
 218 on the larger survey results, but this does not reflect the reality of field campaigns: there are  
 219 usually no more than a few such campaigns for a given basin in a given decade and averaging  
 220 over 1000 hypothetical surveys does not apply.

221 Figure 3b shows that increasing the sample size per fictional survey to 1000 well visits  
 222 generates an underestimate of total emissions 63% of the time, while a size of 10,000 ef-  
 223 fectively captures large-scale behavior. The extremely non-normal distribution of leak sizes  
 224 plays a large role here and intuition developed with normally distributed phenomena may  
 225 be deceiving. In normally distributed phenomena, small sample sizes cause variance but not  
 226 bias, and increasing sample size reduces the variance in the estimated emissions. But with  
 227 our observed contribution of super-emitters, the median estimate of a fictional survey shifts  
 228 strongly to the right as our sample size increases: at 100 well visits the median estimate is  
 229 38% of our estimate, at 1000 visits this increases to 79%, and at 10,000 visits it increases to  
 230 96% of our estimate.

## 231 **Airplane-detectable emitters drive total emissions**

232 While aerial detection technologies have been critiqued for their relatively high minimum  
 233 detection limit, our results suggest an alternative interpretation: the error introduced from  
 234 the small sample sizes feasible with ground campaigns may overwhelm any benefits they get  
 235 from a lower detection threshold. For example, below-minimum-detection-limit emissions  
 236 account for 9% (+4%/-3%) of our study total, suggesting that higher sensitivity would lead  
 237 to only a modest increase in total estimated emissions relative to simulated levels.

238 In conclusion, we conducted a site-level, basin-wide field survey of methane emissions  
 239 in one of the most active oil-producing regions in the world. We estimate emissions to be

240 9.4% (+3.5%/-3.3%) of the gross gas production for the region, much higher than found in  
241 previous studies with overlapping, although not identical, domains. The increase is partly  
242 because our method allows us to inspect the entire O&G-producing population using an  
243 independently-verified instrument capable of detecting large methane emissions. This allows  
244 us to identify the largest emissions from all assets surveyed, sidestepping the statistical  
245 uncertainties of scaling-up small samples of ground-based field measurements.

246 Previous studies rarely observed emissions larger than 10 kg/h at a single site, yet our  
247 basin-wide survey of over 30,000 assets uncovered 1958 methane plumes above this size.<sup>8,13</sup>  
248 This includes many emissions over 100 and 1000 kg/h, with emissions above 308 kg/h ac-  
249 counting for half of measured emissions for the region. While it is possible that the New  
250 Mexico Permian was an anomaly during this study period, the clear impact of large emis-  
251 sions found by this study suggests that estimates from ground-based methane surveys may  
252 be underestimating total emissions by missing low-frequency, high-impact large emissions.

## 253 **Acknowledgments**

254 The authors would like to thank the Kairos Aerospace team for collecting and preparing the  
255 data for this study. The authors gratefully acknowledge the help from Ritesh Gautam, Ben  
256 Hmiel, David Lyon, and Mark Omara at the Environmental Defense Fund, Yuzhong Zhang  
257 currently at Westlake University, Anna Robertson and Shane Murphy at the University of  
258 Wyoming, and Daniel Cusworth and Riley Duren at Carbon Mapper, and Andrew Thorpe at  
259 NASA's Jet Propulsion Lab for assisting in comparing this aerial survey with their methane  
260 studies. The authors would like to thank Jeffrey Rutherford at Stanford University for  
261 providing comments on the study.

## 262 **Author Information**

263 Yuanlei Chen and Evan D. Sherwin contributed equally to this work.

## 264 **Funding Sources**

265 This study was funded by the Stanford Natural Gas Initiative, an industry consortium that  
266 supports independent research at Stanford University. Analysis was supported in part by  
267 the Alfred P. Sloan Foundation Grant G-2019-12451 in support of the Flaring and Fossil  
268 Fuels: Uncovering Emissions and Losses (F3UEL) project.

## 269 **Data availability**

270 The data required to reproduce key results in this article are available at [https://github.com/KairosAerospace/stanford\\_nm\\_data\\_2021](https://github.com/KairosAerospace/stanford_nm_data_2021). While the remaining data from this study  
271 are not available for open release due to confidentiality concerns, Kairos Aerospace is com-  
272 mitted to working with research groups studying methane emissions. Access may be granted,  
273 but must be done directly through Kairos Aerospace. Interested researchers should contact  
274 [research-collaborations@kairosaerospace.com](mailto:research-collaborations@kairosaerospace.com).

## 276 **References**

- 277 (1) U.S. Environmental Protection Agency (EPA), Understanding  
278 Global Warming Potentials. [https://www.epa.gov/ghgemissions/  
279 understanding-global-warming-potentials](https://www.epa.gov/ghgemissions/understanding-global-warming-potentials).
- 280 (2) U.S. Energy Information Administration (EIA), Permian region drilling productivity  
281 report. <https://www.eia.gov/petroleum/drilling/pdf/permian.pdf>, 2020.
- 282 (3) U.S. Energy Information Administration (EIA), Natural gas spot and futures prices  
283 (NYMEX). [https://www.eia.gov/dnav/ng/ng\\_pri\\_fut\\_s1\\_d.htm](https://www.eia.gov/dnav/ng/ng_pri_fut_s1_d.htm).

- 284 (4) U.S. Energy Information Administration (EIA), Permian Basin natural gas prices  
285 up as a new pipeline nears completion. [https://www.eia.gov/naturalgas/weekly/  
286 archivenew\\_ngwu/2020/03\\_19/#tabs-rigs-1](https://www.eia.gov/naturalgas/weekly/archivenew_ngwu/2020/03_19/#tabs-rigs-1), 2019.
- 287 (5) U.S. Department of Energy (DOE), New Mexico natural gas flaring and venting regu-  
288 lations. [https://www.energy.gov/sites/prod/files/2019/08/f66/New%20Mexico.  
289 pdf](https://www.energy.gov/sites/prod/files/2019/08/f66/New%20Mexico.pdf), 2019.
- 290 (6) Zhang, Y.; Gautam, R.; Pandey, S.; Omara, M.; Maasackers, J. D.; Sadavarte, P.;  
291 Lyon, D.; Nesser, H.; Sulprizio, M. P.; Varon, D. J., et al. Quantifying methane emis-  
292 sions from the largest oil-producing basin in the United States from space. *Science  
293 advances* **2020**, *6*, eaaz5120.
- 294 (7) Lyon, D. R.; Hmiel, B.; Gautam, R.; Omara, M.; Roberts, K. A.; Barkley, Z. R.;  
295 Davis, K. J.; Miles, N. L.; Monteiro, V. C.; Richardson, S. J., et al. Concurrent vari-  
296 ation in oil and gas methane emissions and oil price during the COVID-19 pandemic.  
297 *Atmospheric Chemistry and Physics* **2021**, *21*, 6605–6626.
- 298 (8) Robertson, A. M.; Edie, R.; Field, R. A.; Lyon, D.; McVay, R.; Omara, M.; Zavala-  
299 Araiza, D.; Murphy, S. M. New Mexico Permian Basin Measured Well Pad Methane  
300 Emissions Are a Factor of 5–9 Times Higher Than US EPA Estimates. *Environmental  
301 Science & Technology* **2020**,
- 302 (9) Schneising, O.; Buchwitz, M.; Reuter, M.; Vanselow, S.; Bovensmann, H.; Burrows, J. P.  
303 Remote sensing of methane leakage from natural gas and petroleum systems revisited.  
304 *Atmospheric Chemistry and Physics* **2020**, *20*, 9169–9182.
- 305 (10) Cusworth, D. H.; Duren, R. M.; Thorpe, A. K.; Olson-Duvall, W.; Heckler, J.; Chap-  
306 man, J. W.; Eastwood, M. L.; Helmlinger, M. C.; Green, R. O.; Asner, G. P., et al.  
307 Intermittency of Large Methane Emitters in the Permian Basin. *Environmental Science  
308 & Technology Letters* **2021**,

- 309 (11) Alvarez, R. A.; Zavala-Araiza, D.; Lyon, D. R.; Allen, D. T.; Barkley, Z. R.;  
310 Brandt, A. R.; Davis, K. J.; Herndon, S. C.; Jacob, D. J.; Karion, A., et al. As-  
311 sessment of methane emissions from the US oil and gas supply chain. *Science* **2018**,  
312 *361*, 186–188.
- 313 (12) Maasackers, J. D.; Jacob, D. J.; Sulprizio, M. P.; Turner, A. J.; Weitz, M.; Wirth, T.;  
314 Hight, C.; DeFigueiredo, M.; Desai, M.; Schmeltz, R., et al. Gridded national inventory  
315 of US methane emissions. *Environmental science & technology* **2016**, *50*, 13123–13133.
- 316 (13) Omara, M.; Zimmerman, N.; Sullivan, M. R.; Li, X.; Ellis, A.; Cesa, R.; Subrama-  
317 nian, R.; Presto, A. A.; Robinson, A. L. Methane emissions from natural gas produc-  
318 tion sites in the United States: Data synthesis and national estimate. *Environmental*  
319 *science & technology* **2018**, *52*, 12915–12925.
- 320 (14) Rutherford, J. S.; Sherwin, E. D.; Ravikumar, A. P.; Heath, G. A.; Englander, J.; Coo-  
321 ley, D.; Lyon, D.; Omara, M.; Langfitt, Q.; Brandt, A. R. Closing the gap: Explaining  
322 persistent underestimation by US oil and natural gas production-segment methane in-  
323 ventories [Preprint]. <https://doi.org/10.31223/X5JC7T>, 2020.
- 324 (15) Brandt, A. R.; Heath, G.; Kort, E.; O’Sullivan, F.; Pétron, G.; Jordaan, S. M.; Tans, P.;  
325 Wilcox, J.; Gopstein, A.; Arent, D., et al. Methane leaks from North American natural  
326 gas systems. *Science* **2014**, *343*, 733–735.
- 327 (16) Kairos Aerospace, Technical White Paper: Methane Detection. 2019.
- 328 (17) U.S. Energy Information Administration (EIA), Maps: Oil and Gas Exploration, Re-  
329 sources, and Production. <https://www.eia.gov/maps/maps.htm>.
- 330 (18) Sherwin, E. D.; Chen, Y.; Ravikumar, A. P.; Brandt, A. R. Single-blind test of airplane-  
331 based hyperspectral methane detection via controlled releases. *Elementa: Science of the*  
332 *Anthropocene* **2021**, *9*.



- 333 (19) Duren, R. M. et al. California's methane super-emitters. *Nature* **2019**, *575*, 180–184.
- 334 (20) Dark Sky by Apple Inc., Dark Sky data attribution. [https://darksky.net/](https://darksky.net/attribution)  
335 [attribution](https://darksky.net/attribution).
- 336 (21) Jones, B. B.; Dieker, S. W. Systems and methods for detecting gas leaks. 2019;  
337 [http://patft.uspto.gov/netacgi/nph-Parser?Sect1=PT02&Sect2=HITOFF&p=1&](http://patft.uspto.gov/netacgi/nph-Parser?Sect1=PT02&Sect2=HITOFF&p=1&u=%2Fmetahtml%2FPT0%2Fsearch-bool.html&r=1&f=G&l=50&co1=AND&d=PTXT&s1=10267729&OS=10267729&RS=10267729)  
338 [u=%2Fmetahtml%2FPT0%2Fsearch-bool.html&r=1&f=G&l=50&co1=AND&d=PTXT&s1=](http://patft.uspto.gov/netacgi/nph-Parser?Sect1=PT02&Sect2=HITOFF&p=1&u=%2Fmetahtml%2FPT0%2Fsearch-bool.html&r=1&f=G&l=50&co1=AND&d=PTXT&s1=10267729&OS=10267729&RS=10267729)  
339 [10267729&OS=10267729&RS=10267729](http://patft.uspto.gov/netacgi/nph-Parser?Sect1=PT02&Sect2=HITOFF&p=1&u=%2Fmetahtml%2FPT0%2Fsearch-bool.html&r=1&f=G&l=50&co1=AND&d=PTXT&s1=10267729&OS=10267729&RS=10267729).
- 340 (22) Kairos Aerospace, Methane Emissions Quantification.  
341 [https://kairosaerospace.com/wp-content/uploads/2020/12/](https://kairosaerospace.com/wp-content/uploads/2020/12/Kairos-Emissions-Quantification-20201218.pdf)  
342 [Kairos-Emissions-Quantification-20201218.pdf](https://kairosaerospace.com/wp-content/uploads/2020/12/Kairos-Emissions-Quantification-20201218.pdf), 2020.
- 343 (23) Ravikumar, A. P.; Sreedhara, S.; Wang, J.; Englander, J.; Roda-Stuart, D.; Bell, C.;  
344 Zimmerle, D.; Lyon, D.; Mogstad, I.; Ratner, B., et al. Single-blind inter-comparison  
345 of methane detection technologies—results from the Stanford/EDF Mobile Monitoring  
346 Challenge. *Elementa: Science of the Anthropocene* **2019**, *7*.
- 347 (24) Bañuelos-Ruedas, F.; Camacho, C. Á.; Rios-Marcuello, S. Methodologies used in the  
348 extrapolation of wind speed data at different heights and its impact in the wind energy  
349 resource assessment in a region. *Wind farm-technical regulations, potential estimation*  
350 *and siting assessment* **2011**, 97–114.
- 351 (25) Grossman, A. Dark Sky Has a New Home. [https://blog.darksky.net/](https://blog.darksky.net/dark-sky-has-a-new-home/#:~:text=By%20Adam%20Grossman%20on%20August,be%20receiving%20a%20full%20refund.)  
352 [dark-sky-has-a-new-home/#:~:text=By%20Adam%20Grossman%20on%20](https://blog.darksky.net/dark-sky-has-a-new-home/#:~:text=By%20Adam%20Grossman%20on%20August,be%20receiving%20a%20full%20refund.)  
353 [%20August,be%20receiving%20a%20full%20refund.](https://blog.darksky.net/dark-sky-has-a-new-home/#:~:text=By%20Adam%20Grossman%20on%20August,be%20receiving%20a%20full%20refund.), 2020.
- 354 (26) HRRR archive at the University of Utah. [http://home.chpc.utah.edu/~u0553130/](http://home.chpc.utah.edu/~u0553130/Brian_Blaylock/)  
355 [Brian\\_Blaylock/](http://home.chpc.utah.edu/~u0553130/Brian_Blaylock/).

- 356 (27) Ravikumar, A. P.; Wang, J.; McGuire, M.; Bell, C. S.; Zimmerle, D.; Brandt, A. R.  
357 “Good versus good enough?” Empirical tests of methane leak detection sensitivity of a  
358 commercial infrared camera. *Environmental science & technology* **2018**, *52*, 2368–2374.
- 359 (28) Eastern Research Group, City of Fort Worth natural gas air quality study.  
360 [https://www.fortworthtexas.gov/departments/development-services/  
361 gaswells/air-quality-study/final](https://www.fortworthtexas.gov/departments/development-services/gaswells/air-quality-study/final), 2011.
- 362 (29) Environmental Defense Fund, Permian Methane Analysis Project (PermianMAP).  
363 <https://www.permianmap.org/>.
- 364 (30) Royal Netherlands Meteorological Institute, TROPOMI methane data product. [http:  
365 //www.tropomi.eu/data-products/methane](http://www.tropomi.eu/data-products/methane).
- 366 (31) GHGSat, GHGSat global emissions monitoring services. [https://www.ghgsat.com/  
367 data-products-analytics/](https://www.ghgsat.com/data-products-analytics/).
- 368 (32) European Space Agency, About GOSAT-2. [https://earth.esa.int/eogateway/  
369 missions/gosat-2?text=methane](https://earth.esa.int/eogateway/missions/gosat-2?text=methane).
- 370 (33) Enverus, Exploration and Production. [https://www.enverus.com/industry/  
371 exploration-and-production/](https://www.enverus.com/industry/exploration-and-production/).
- 372 (34) National Oceanic and Atmospheric Administration (NOAA), High Resolution Rapid  
373 Refresh (HRRR) CONUS 2-D Fields GRIB2 table documentation. [https://  
374 rapidrefresh.noaa.gov/hrrr/HRRRv4\\_GRIB2\\_WRFTWO.txt](https://rapidrefresh.noaa.gov/hrrr/HRRRv4_GRIB2_WRFTWO.txt), 2020.
- 375 (35) Environmental Defense Fund, New Data: Permian Oil & Gas Producers Re-  
376 leasing Methane at Three Times National Rate. [https://www.edf.org/media/  
377 new-data-permian-oil-gas-producers-releasing-methane-three-times-national-rate](https://www.edf.org/media/new-data-permian-oil-gas-producers-releasing-methane-three-times-national-rate).
- 378 (36) Rohatgi, A. Webplotdigitizer: Version 4.4. 2020; [https://automeris.io/  
379 WebPlotDigitizer](https://automeris.io/WebPlotDigitizer).

380 **Disclosures**

381 Elena S.F. Berman, Brian B. Jones, Matthew P. Gordon, and Erin B. Wetherley are em-  
382 ployees of Kairos Aerospace. The remaining authors have no competing interests to declare.